IOPscience iopscience.iop.org

Home Search Collections Journals About Contact us My IOPscience

Development of ReflEXAFS data analysis for deeper surface structure studies

This content has been downloaded from IOPscience. Please scroll down to see the full text.

2009 J. Phys.: Conf. Ser. 190 012110

(http://iopscience.iop.org/1742-6596/190/1/012110)

View the table of contents for this issue, or go to the journal homepage for more

Download details:

IP Address: 150.214.9.250
This content was downloaded on 31/07/2017 at 12:37

Please note that terms and conditions apply.

You may also be interested in:

Exafs and comparative studies of copper (II) complexes
A Mishra and S Mishra

Application of XAFS to Catalytic Materials
Gilberto Vlaic, Emiliano Fonda, Rinaldo Psaro et al.

Femtometer accuracy EXAFS measurements: Isotopic effect in the first, second and third coordination shells of germanium
J Purans, J Timoshenko, A Kuzmin et al.

Site of Sulfur Impurities in Silicate Glasses and ReflEXAFS Studies around the Si K-edge
P. Lagarde, R. Delaunay, A.-M. Flank et al.

Effects of a Metal Film and Prism Dielectric on Properties of Surface Plasmon Resonance in a Multilayer System
Chin-Hsiung Liao, Cheng-Min Lee, Liann-Be Chang et al.

Linking Monte-Carlo simulation and target transformation factor analysis: a novel tool for the EXAFS analysis of mixtures
A Rossberg and A Scheinost

Structural and Magnetic Properties of Codoped ZnO based Diluted Magnetic Semiconductors
Li Bin-Bin, Shen Hong-Lie, Zhang Rong et al.

Effects of Added Metallic Elements in Ag-Alloys on Properties of Indium–Tin-Oxide/Ag-Alloy/Indium–Tin-Oxide Transparent Conductive Multilayer System
Hee-Sook Roh, Geun-Hong Kim and Won-Jong Lee

Development of ReflEXAFS data analysis for deeper surface structure studies

Víctor López-Flores[1,*], Stuart Ansell[2], Silvia Ramos[3], Daniel T. Bowron[2], Sofía Díaz-Moreno[3], and Adela Muñoz-Páez[1]

E-mail: *`victor.lopez@icmse.csic.es`
[1]Institute of Materials Science of Seville, Inorganic Chemistry Department (CSIC – University of Seville), 41092 Seville, Spain; [2]ISIS Facility, Rutherford Appleton Laboratory, Chilton, Didcot, Oxfordshire OX11 0QX, U.K.; [3]Diamond Light Source Ltd., Harwell Science and Innovation Campus, Didcot, Oxfordshire, OX11 0DE, U.K.

Abstract. An analytical approach to the analysis of ReflEXAFS data collected from complex multilayer samples, at a range of angles above and below the critical angle is presented. The aim of the technique is to generate a structural model of the investigated system that is consistent with the variable depth sensitivity of the experimental data. The procedure follows three main steps (i) the determination of the free atom reflectivity background for the multilayer system, (ii) the estimation of the depth dependent EXAFS signals and (iii) the calculation of the corresponding ReflEXAFS components. By iterating between steps (ii) and (iii), and varying the estimates of the EXAFS signals, a consistent set of structural parameters is extracted that reflects the bulk structure of the multilayer system through the basic reflectivity signals, and the depth dependent local atomic structure through the estimated EXAFS components. An example of the depth dependent structure of copper in a copper-chromium multilayer stack is presented to illustrate the capabilities of the method.

1. Introduction

Extended X ray Absorption Fine Structure spectroscopy (EXAFS) is a well established method to determine the local atomic environment of a selected element in a wide variety of samples [1]. From both a scientific and industrial perspective, there has been a significant increase in interest about the properties of surfaces and interfaces lately. A way of achieving surface sensitivity is to record the intensity of the reflected beam from a flat surface. This detection mode is called reflection EXAFS, or ReflEXAFS [2]. The novelty and main advantage of this technique is that it provides a method to control the depth at which the sample is being probed. For incidence angles below the critical angle (total reflection regime), only a few Ångströms below the surface are probed by an evanescent wave. For incidence angles above the critical angle, the penetration depth of the radiation, and thus the probed depth in the sample, increases continuously with the angle. However, until recently it has been used mostly under the total reflection regime, for two main reasons: (1) experimental difficulties, and (2) difficulties in data analysis. In a previous paper [3] we described the development of an automated set-up and protocols to carry out high quality ReflEXAFS experiments both in total and non-total reflection regime, and how they can be implemented in a beamline at a third generation synchrotron radiation source. The analysis of the ReflEXAFS spectra for incidence angles not in the total reflection regime differ considerably from the standard EXAFS analysis for several reasons, so the standard procedure cannot be applied. A few studies [4, 5] have gone beyond the total reflection approximation, but suffer from some strong restrictions. In this paper we present a method to analyse ReflEXAFS spectra recorded below and above the critical angle of reflection, which we hope will help to unlock the full potential of the technique as a structural probe with chemical and depth selectivity.

© 2009 IOP Publishing Ltd

Journal of Physics: Conference Series **190** (2009) 012110 doi:10.1088/1742-6596/190/1/012110

2. Method

The refractive index of a material in the X ray energy region is normally written as [6] $n(E) = 1 - \delta(E) - i\beta(E)$. A reflectivity spectrum is a function of both the real and imaginary parts of the refractive index $R(E) = R[\delta(E), \beta(E)]$. By definition, the ReflEXAFS signal of a reflectivity spectrum as a function of energy is small compared to the reflectivity itself. Then, the fine structure can be expanded in terms of $\delta(E)$ and $\beta(E)$ to a linear approximation, giving [7]

$$R[\delta(E), \beta(E)] - R_0[\delta_0(E), \beta_0(E)] = \Delta R(E) \approx \left.\frac{\partial R}{\partial \delta}\right|_{\delta_0} \Delta\delta(E) + \left.\frac{\partial R}{\partial \beta}\right|_{\beta_0} \Delta\beta(E)\,, \tag{1}$$

where R_0 represents the reflectivity curve for the sample without the fine structure, or free atom reflectivity. The functions $\delta(E)$ and $\beta(E)$ can also be written as a sum of the free atom and fine structure functions as: $\delta(E) = \delta_0(E) + \Delta\delta(E)$, $\beta(E) = \beta_0(E) + \Delta\beta(E)$.

Eq. (1) is the starting point of all the data analysis methods of the ReflEXAFS signal. It is at this level that some of them have made approximations that simplified the problem [2, 4, 5]. All of these preceding methods obtain the EXAFS signal from the ReflEXAFS signal measured at individual angles. In contrast, the principles of the method presented here are: (i) to work over a complete set of measurements of the same sample in the same energy range, but at different incidence angles; (ii) to avoid extracting the EXAFS signal from a spectrum at a particular incidence angle, but instead, propose the EXAFS signals of the different EXAFS environments present at the sample (for instance, at different layers), and then calculate the corresponding ReflEXAFS signal of each spectrum at the different incidence angles, so they can be fitted against the experimental signals; (iii) to obtain the EXAFS signal of the sample local atomic environment or environments that can be analyzed by conventional methods.

This procedure requires two processes to deliver a global and local structure solution. First, a free atom reflectivity simulation and fit is performed for all the spectra of the sample at different angles. Second, the ReflEXAFS signal is fitted against a model function representing the EXAFS signal of the local environments studied [8].

2.1. Free atom reflectivity simulation and fit

To calculate the free atom reflectivity, $R_0(E) = R_0\left[\delta_0(E), \beta_0(E)\right]$, a model of the sample is built. As an example, consider a sample made of homogeneous layers of different materials deposited over a certain substrate. For this type of sample, the free atom reflectivity can be rewritten as $R_{0m}(E) = R_{0m}\left[\delta_{0j}(E), \beta_{0j}(E)\right]$, where $m \in \{1, \ldots, M\}$ denotes the spectrum recorded for this sample at each different incidence angle and $j \in \{0, \ldots, N+1\}$ denotes the different layers. Layer 0 is the incidence material (air of vacuum) and layer $N+1$ the semi-infinite substrate.

The reflectivity spectra are functions of the refractive index components for the free atom, $\delta_{0j}(E)$ and $\beta_{0j}(E)$, for each j-th layer, which can be obtained from the tabulated values of the anomalous scattering factors of, for instance, the Henke [9] tables. These functions depend on the chemical composition and atomic density of the layer components. The reflectivity spectra at different energies for each $(j-1, j)$ interface can then be calculated using the parameters described above in the recursive expression [10]

$$r'_{j-1,j} = r_{j-1,j} + \frac{t_{j-1,j}t_{j,j-1}r'_{j,j+1}e^{-i\phi_j(E) - D_j\mu_j(E)}}{1 + r_{j-1,j}r'_{j,j+1}e^{-i\phi_j(E) - D_j\mu_j(E)}}\,. \tag{2}$$

where r and t are the Parratt [6] approximations of the Fresnel reflection and transmission coefficients for X rays at small grazing angles. $\phi_j(E) = \frac{4\pi d_j \sin(\theta_j)}{\lambda(E)} = \frac{2Ed_j \sin(\theta_j)}{\hbar c}$ is the phase difference between the different reflections caused by the path length difference, and $e^{-D_j\mu_j(E)}$ is the attenuation term of the wave traveling through the material whose absorption coefficient is $\mu_j(E)$, where $D_j = \frac{2d_j}{\sin(\theta_j)}$ is the total path travelled by the beam in layer j, of thickness d_j. $\lambda(E)$ is the wavelength of the radiation, θ_j is the angle of the beam at layer j. This expression is not the usual Parratt recursion formula [6] where the Stokes relationship, $t_{j-1,j}t_{j,j-1} = 1 - r^2_{j-1,j}$,

is used. This is only valid if there is no absorption in the material, which is not the case in a ReflEXAFS spectrum, and this calculation needs the evaluation of each $r_{j-1,j}$, starting from the substrate, where $r_{N+1,N+2} = 0$. As the aim of the method is the analysis of experimental data, a roughness correction [11] is also required.

The sample characteristics, (density, thickness and roughness of the layers), the incidence angle and an energy shift correction are then set as variables in a simulation that fits the calculated reflectivity against the experimental data. Once performed, the fitting procedure provides precise values of the refractive index components of the layers without the fine structure, $\delta_{0j}(E)$ and $\beta_{0j}(E)$. These values will be of paramount importance for the subsequent simulation of the ReflEXAFS signal. Also, after the fitting, it is possible to extract the ReflEXAFS signal from each spectrum, $\Delta R_m(E)$.

The idea behind the method described above is simple. However, the fitting procedure is challenging due to the large number of parameters involved. Also, the magnitude of some partial reflectivities may be so small that its calculation may suffer from rounding errors that are magnified during the simulation (ill-conditioning problems). Moreover, the noise and possible glitches of the experimental spectra adds a further complication to the simulation. To overcome these problems, two main strategies are adopted. First, volume of parameter space is reduced by using approximate knowledge of key variables obtained from other sources such as AFM studies of surface roughness. Second, as many variables as possible are linked together such as thicknesses in a multilayer. After this, all the experimental reflectivity spectra that were taken at different angles, are simulated and the fitting of the reflectivity curves is performed using the sophisticated algorithm known as the *Covariance Matrix Adaptation Evolution Strategy* or CMA-ES algorithm [12] This is a type of evolutionary algorithm well suited to the problem as it has been specifically designed for simulations that have (i) high dimensionality (ii) ruggedness, (iii) noisy data and discontinuities, (iv) ill-conditioning problems.

2.2. ReflEXAFS simulation and fit

Continuing with the layered sample case, there is a total of $N+1$ layers, including the substrate. However, the number of layers that contain the absorbing element whose absorption edge is being studied, that will be denoted H, could be smaller than the total number of layers, i.e. $1 \leq H \leq N+1$. Thus, the contribution to the fine structure of the reflectivity can only come from the fine structures of those layers, so $\Delta R_m(E) = \Delta R_m\left[\Delta\delta_h(E), \Delta\beta_h(E)\right]$ where $h \in \{1, \ldots, H\}$ denotes only the layers that contain the absorbing element, where each absorbing layer h may have a different fine structure spectrum. Then, the expansion of Eq. (1) has to be made for all possible contributions from each layer h, so

$$\Delta R_m(E) \approx \sum_{h=1}^{H} \left[\left.\frac{\partial R_m}{\partial \delta_h}\right|_{\delta_{0h}} \Delta\delta_h(E) + \left.\frac{\partial R_m}{\partial \beta_h}\right|_{\beta_{0h}} \Delta\beta_h(E) \right] \implies \tag{3}$$

$$\implies \begin{pmatrix} \Delta R_1(E) \\ \vdots \\ \Delta R_M(E) \end{pmatrix} \approx \begin{pmatrix} \frac{\partial R_1}{\partial \delta_1}\big|_{\delta_{01}} & \frac{\partial R_1}{\partial \beta_1}\big|_{\beta_{01}} & \cdots & \frac{\partial R_1}{\partial \delta_H}\big|_{\delta_{0H}} & \frac{\partial R_1}{\partial \beta_H}\big|_{\beta_{0H}} \\ \vdots & \vdots & \ddots & \vdots & \vdots \\ \frac{\partial R_M}{\partial \delta_1}\big|_{\delta_{01}} & \frac{\partial R_M}{\partial \beta_1}\big|_{\beta_{01}} & \cdots & \frac{\partial R_M}{\partial \delta_H}\big|_{\delta_{0H}} & \frac{\partial R_M}{\partial \beta_H}\big|_{\beta_{0H}} \end{pmatrix} \begin{pmatrix} \Delta\delta_1(E) \\ \Delta\beta_1(E) \\ \vdots \\ \Delta\delta_H(E) \\ \Delta\beta_H(E) \end{pmatrix}, \tag{4}$$

where each of the partial derivatives are explicit functions of E. In words, this means that the reflectivity fine structure at each individual energy point can be approximated by a linear combination of the fine structures of the real and imaginary components of the refractive indices of all the absorbing layers. This equation is valid for each m spectrum, with its own partial derivative coefficients, but shares the same $\Delta\delta_h(E)$ and $\Delta\beta_h(E)$, which are characteristic of the layers, but not the spectrum. This form a linear set of equations where the coefficient matrix, $A(E)$ is a rectangular $M \times 2H$ matrix, that defines a different set for each energy point.

The method used to solve these equations is to assume $\Delta\mu_h(E)$ is a set of independent points, one for each energy value. Then, $\Delta\beta_h(E)$ is calculated by $\mu(E) = \frac{2E}{\hbar c}\beta(E)$ and $\Delta\delta_h(E)$

is calculated by the Kramers-Kronig relationship [4]. Once these functions have been calculated, the coefficients of matrix $A(E)$ can be calculated by a numerical derivative. With these coefficients, the equation can be solved by the evaluation of the Moore-Penrose *pseudoinverse*, $A^{+}(E)$, of matrix $A(E)$ for each energy point, which gives the least squares solution of the system of equations [13]. The solution of the equation thus obtained for each energy point is a new and different set of points that describe $\Delta\delta_h(E)$ and $\Delta\beta_h(E)$. These new functions can be used again to calculate the coefficients of matrix $A(E)$ by a numerical derivative, so the process can start again. This process is then done iteratively until the difference between the $\Delta\delta_h(E)$ and $\Delta\beta_h(E)$ functions between two consecutive steps is small.

This method has some problems if some of the matrix elements of $A(E)$ are too small, as they will have rounding errors in a computer that will be magnified in the calculation of the pseudoinverse. To overcome this issue, it is convenient to use an orthogonal decomposition method for the calculation of the pseudoinverse. Specifically, the *Singular Value Decomposition* or *SVD* method was used in this work, as it is possible to use the truncated matrices approximation to avoid these rounding errors [14]. In many cases, the above approach did not converge and oscillated, but empirical tests have shown that a means to stabilize the inversion of the matrix was to simultaneously work with its Kramers-Kronig inverted form

$$\mathcal{KK}\left[\Delta R_m(E)\right] \approx \sum_{h=1}^{H} \left\{ -\mathcal{KK}\left[\left.\frac{\partial R_m}{\partial \delta_h}\right|_{\delta_{0h}} \right] \Delta\beta_h(E) + \mathcal{KK}\left[\left.\frac{\partial R_m}{\partial \beta_h}\right|_{\beta_{0h}} \right] \Delta\delta_h(E) \right\} , \qquad (5)$$

This way, the equation has a double constraint. The resulting $\Delta\beta_h(E)$ are normalised to the $\beta_{0h}(E)$ jump so, finally, each $\mu_h(E)$ can be calculated using the relationship $\mu(E) = \frac{2E}{\hbar c}\beta(E)$, and may then be analysed using the standard EXAFS analysis programs [15, 16]

3. Example

As an example of application of the method, the complete ReflEXAFS analysis of a multilayered sample is presented here. The aim is to successfully apply the above described method to extract and analyse ReflEXAFS data from buried layers, and compare the results with a total reflection approximation analysis. The sample is a $(CuCr)_8$ multilayer, grown over a monocrystalline Si (100) wafer, to ensure flatness, by Direct Current Magnetron Sputtering Physical Vapor Deposition. The characterisation showed [17] that the sample is composed of a bilayer of Cu and Cr of 18 and 10 Å respectively, repeated 8 times. Both Cu and Cr layers keep the densities of the bulk crystalline metals. The surface roughness is about 14 Å. Furthermore, the surface topography image taken by Atomic Force Microscopy AFM shows a set of emerging columns with a base of about 100 nm wide, scattered randomly across the surface.

The ReflEXAFS measurements were performed as explained in our previous report [3]. The set of experimental spectra are shown in solid line in Fig. 1.I. The spectra may be analyzed by using either the total reflection approximation [2] for the lowest incidence angle, which will give information concerning only the first Cu layer, or the global analysis method described in this work for the whole set of incidence angles that will provide us with information about all the layers in the sample, as the penetration depth for the highest incidence angle spectrum of the set is larger than the total thickness. In principle, the local environment of the Cu atoms in all the layers should be the same, as the growing conditions are identical. However, differences are expected due to the small thickness of the layers.

The free atom reflectivity simulation and fit of the experimental spectra was performed with a program written in C++ that follows the algorithm described in section 2.1. The variables of the fit are the thicknesses and densities of the layers and the roughnesses of the interfaces, linked in an appropiate manner to describe the sample symmetry. Each spectrum has its incidence angle as independent variable, while the energy shift correction was set to be the same for all spectra. The results of the free atom reflectivity fit agree with the previous sample characterization.

The global ReflEXAFS was extracted using the simulation method described in section 2.2 assuming the same EXAFS environment for all the layers in the sample. Fig. 1.I shows the

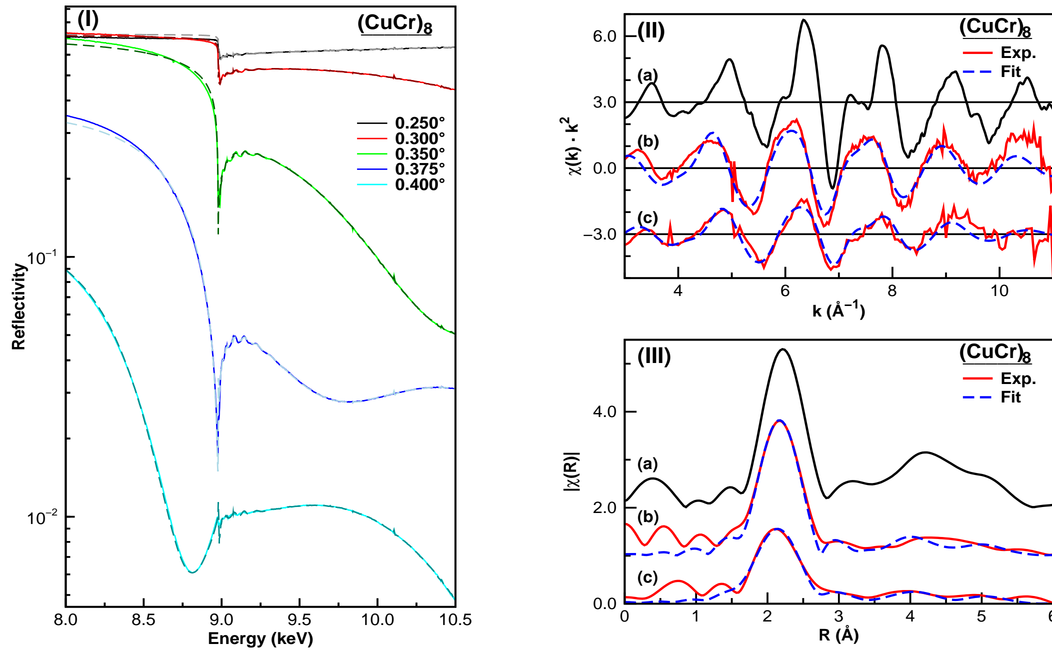

Figure 1: (I) ReflEXAFS experimental spectra (solid) and best fit (dashed) for sample $(CuCr)_8$. (II) EXAFS experimental χ(k) for (IIa) a Cu foil reference and experimental with their best fits for (IIb) global analysis, (IIc) total reflection approximation. (III) EXAFS experimental χ(R) for (IIIa) a Cu foil reference and experimental with their best fits for (IIIb) global analysis, (IIIc) total reflection approximation

best fit complete reflectivity simulated spectra in dashed lines, where the fine structure has been added to the previously simulated free atom reflectivity. The lowest incidence angle fine structure (0.250°) was extracted by conventional methods, using the program AUTOBK [16].

For both EXAFS analysis, the IFEFFIT [18] suite was used. Both signals were simulated and fitted by using a Cu metal model structure with coordination numbers fixed to the crystal values. A single free parameter, Δa, varying the lattice parameter from the Cu bulk value (3.61 Å) was used to allow the variation of coordination distances coherently for all the coordination shells of the model. Moreover, the Debye-Waller factors, σ^2, were allowed to vary independently for each shell and S_0^2 was set to 0.81. Only the single scattering paths of up to the 5th shell and the colinear multiple scattering paths of the 4th shell (using both the same Debye-Waller factor as the 4th shell simple scattering path) were used. Tab. 1 shows the best fit variables of the simulation for both the total reflection and the global analyses. Fig. 1.II shows the EXAFS signal of both analyses with their respective best fits, with a Cu metal reference, in the wavevector space, while Fig. 1.III shows the Fourier transform magnitude of the same signals.

Table 1: EXAFS analysis results for $(CuCr)_8$ sample. Errors indicated in brackets

Method	Shell (N)	1^{st}(12)	2^{nd}(6)	3^{rd}(24)	4^{th}(12)	5^{th}(24)	Δa(Å)	ΔE(eV)
Global	**R (Å)**	2.55(1)	3.60(1)	4.42(2)	5.09(2)	5.70(2)	-0.01(1)	-5.8 (1.7)
	σ^2 **(Å^2)**	0.008(1)	0.019(8)	0.021(6)	0.021(4)	0.02(2)		
Total Reflec.	**R (Å)**	2.51(2)	3.55(2)	4.35(3)	5.03(3)	5.62(3)	-0.06(2)	-3.3 (1.9)
	σ^2 **(Å^2)**	0.015(1)	0.018(10)	0.026(9)	0.026(7)	0.03(3)		

The results from both methods show that all the layers in the sample maintain the Cu metal environment. However, the high values of the Debye-Waller factors suggest that this environment is extremely disordered compared to the crystalline environment in a metal foil. This is a consequence of the low thickness of the layers, that prevents a full reorganization of the atoms once grown on the substrate by the magnetron sputtering deposition technique used to prepare the sample [17]. The slight compression of the lattice parameter may arise from

the interdiffusion of the Cr atoms of the alternating layers, that reduces the bonding distances due to the smaller Cr-Cu distance. At the same time, the crystal lattice of Cr may be slightly distorting the Cu lattice [19].

There is a quantitative difference between the total reflection approximation and the global method that is a consequence of a difference between the topmost Cu layer and the rest of them. A hint of a peak at approximately the Cu-O distance can be seen at 1.3 Å in the Fourier Transform magnitude plot of the total reflection approximation spectrum, although it is not sufficiently resolved to be analyzable. If the Cr cover layer is not thick enough to protect the first Cu layer, oxygen can penetrate and oxidize the latter. This oxidation can be so small that a well resolved Cu-O first shell peak might not be seen. However, the second Cu oxide peak (Cu-Cu) may be significant enough to interfere with the first Cu metal shell peak, so it can distort and displace it to lower R values. The first Cu layer can be non-uniformly oxidized due to the local variation of thicknesses that can occur in the first Cr layer. Then, the Cu oxide grows preferentially in some spots, emerging from the layer underneath.

This effect does not appear in the global analysis spectrum, so it can be concluded that the rest of the layers are not oxidized. As the global analysis probes all the Cu layers, mostly non-oxidized, the amount of top oxide is negligible, so the spectrum appears as just metallic Cu.

4. Conclusions

In this paper we have described a method to extract the EXAFS signal from a set of ReflEXAFS spectra taken at different incidence angles, both below and above the critical angle of total reflection. The developed algorithm was designed to work for spectra collected from layered samples as this is one of the main fields of application of the ReflEXAFS technique. Homogeneous samples can be studied by other well established EXAFS methods. Specifically, it has been shown that buried layers can be probed and the EXAFS signals can be extracted from differing structural environments as a function of depth. The heart of the approach is to estimate a consistent set of EXAFS signals that come from each layer in the sample, instead of the standard approach of trying to extract a signal for each experimental spectrum measured at differing angles. As an example study the structural differences in the copper environment between the top and the buried layers of a $(CuCr)_8$ multilayer have been evaluated.

References

[1] Teo B K 1986 *EXAFS: Basic principles and data analysis* (Berlin: Springer)
[2] Martens G and Rabe P 1981 *J. Phys. C* **14** 1523–1534
[3] López-Flores V, Ansell S, Bowron D T, Díaz-Moreno S, Ramos S and Muñoz-Páez A 2007 *Rev. Sci. Instrum.* **78** 013109–(1–12)
[4] Borthen P and Strehblow H H 1995 *J. Phys.: Condens. Matter* **7** 3779–3787
[5] Benzi F, Davoli I, Rovezzi M and d'Acapito F 2008 *Rev. Sci. Instrum.* **79** 103902
[6] Parratt L G 1954 *Phys. Rev.* **95** 359–369
[7] Heald S M, Chen H and Tranquada J M 1988 *Phys. Rev. B* **38** 1016–1026
[8] Enquiries regarding the details of the formulation and implementation of the analysis scheme should be directed to stuart.ansell@stfc.ac.uk
[9] Henke B L, Gullikson E M and Davis J C 1993 *Atom. Data Nuc. Data Tab.* **55** 349
[10] Hamley I W and Pedersen J S 1994 *J. Appl. Cryst.* **27** 29–35
[11] Bahr D, Press W, Jebasinski R and Mantl S 1993 *Phys. Rev. B* **47** 4385–4393
[12] Hansen N, Müller S D and Koumoutsakos P 2003 *Evol.Comp.* **11** 1–18
[13] Penrose R 1956 *Proc. Cambr. Phil. Soc.* **52** 17–19
[14] Demmel J and Kahan W 1990 *SIAM J. Sci. and Stat. Comput* **11** 873–912
[15] Rehr J J, De Leon J M, Zabinsky S I and Albers R C 1991 *J. Am. Chem. Soc.* **113** 5135–5140
[16] Newville M, Ravel B, Haskel D, Rehr J J, Stern E A and Yacoby Y 1995 *Physica B* **209** 154–156
[17] López-Flores V, Ansell S, Díaz-Moreno S, Ramos S, Bowron D T, Vila M, García-López J and Muñoz-Páez A 2009 unpublished
[18] Newville M 2001 *J. Sync. Rad.* **8** 322–324
[19] Somorjai G A and Van Hove M A 1979 Adsorbed monolayers on solid surfaces *Structure and bonding* vol 38 (Berlin: Springer-Verlag)